United States Department of Agriculture reference ultraviolet spectroradiometer: current performance and operational experience at Table Mountain, Colorado

Lee Harrison
Jerry Berndt
Piotr Kiedron
State University of New York, Albany
Atmospheric Sciences Research Center
251 Fuller Road
Albany, New York 12203

Patrick Disterhoft
National Oceanographic and Atmospheric
 Administration
Solar Radiation and Research Branch
Central Ultraviolet Calibration Facility
325 Broadway
Boulder, Colorado 80303-3328

Abstract. At present the United States Department of Agriculture (USDA) Reference Spectroradiometric Network consists of three sites: Table Mountain, Colorado, Lamont, Oklahoma (the ARM program SGP site), and Beltsville, Maryland. At each site we deploy and continuously operate a 1-m cascaded additive-double Czerny-Turner scanning monochromator with a bialkali photomultiplier and photon-counting detection. Lambertian fore-optic errors are less than 1% over the range of zenith angles from 0 to 80°. The instruments use photon counting and make measurements at 290 nm not affected by stray light under typical conditions. The basic performance specifications of the instrument were demonstrated by a prototype at the 1997 North-American UV Spectroradiometer Intercomparison. Data shown here demonstrate that these are met in routine operation. The fundamental instrument performance specifications are: Optical resolution: 0.1 nm FWHM, triangular slit-function. Wavelength reproducibility: ± 0.0025-nm 2σ with 296-nm Hg retrace-scan corrections applied, ± 0.007 nm 2σ over typical diurnal variability, without correction. Wavelength accuracy: Limited by calibration systematic errors. Believed to be 0.005-nm worst case. Stray light: $<10^{-7}$ at 4 FWHM, 10^{-10} at 20 nm, slit-scattering function versus 325 nm HeCd. Angular response: less than 1% error from cosine over the range of zenith angles from 0 to 80°. Signal linearity: The instrument uses a photomultiplier with 2-ns rise-time and photon counting detection. The dual-threshold discriminator has a 700-Mhz synchronous signal counting limit. The maximum counting rates seen at the longest wavelengths are less than 10 MHz; less than 1/5 of the frequency where nonlinearity can be detected, as tested for the 1997 Intercomparison. 2000 was the first full year of operation of our instrument at the NOAA Table Mountain site (140.177 °N 105.276 °W, 1900 m asl) for which the operational and calibration frequencies justify making the data accessible to outside users for scientific application. We show performance in routine operation and issues of calibration over the period April 2000 to 31 December 2001. © *2002 Society of Photo-Optical Instrumentation Engineers.*
[DOI: 10.1117/1.1517574]

Subject terms: ultraviolet; radiometers; ozone; remote sensing.

1 Introduction

Measurement of terrestrial ultraviolet spectral irradiance has become a matter of increased scientific interest with the concern over anthropogenic chemicals reducing stratospheric ozone concentrations. Measurements are made both at the surface, and estimated from satellite measurements, the latter to better understand global distributions and impacts.[1–3] A major goal has been understanding both large-geographical-scale and regional differences in surface UV fluxes, and their causes, and to use the ground-based measurements to better calibrate the results of remote sensing.[4–6]

Accurate measurements of the ultraviolet at the Earth's surface for wavelengths 290 to 325 nm (the UVB domain, where the absorption of ozone dominates the atmospheric transmission) are difficult, and have been a persistent problem for both instrument development and calibration.[7,8] The goal of intercomparing data taken by differing instruments, and the need to understand the contributing mechanisms of systematic error have led to instrument intercomparisons; the most recent of a European series is reported.[9] Our instrument participated in the 1997 North American UV spectroradiometer Intercomparison.[10] Brewer spectroradiometers (which are by far the most numerous ultravio-
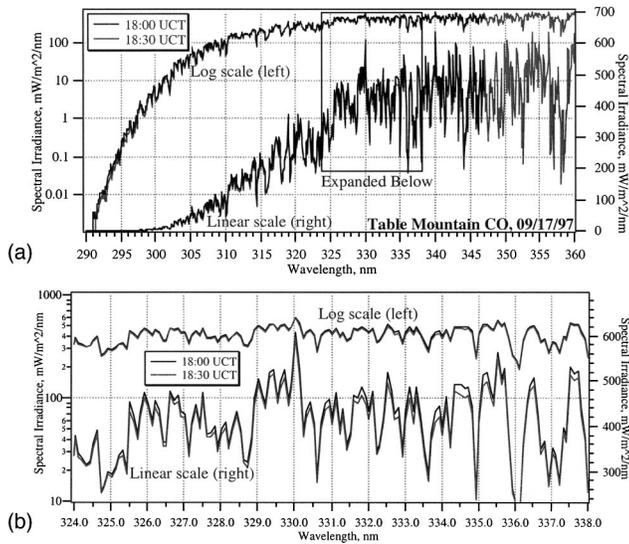
Fig. 1 Spectra taken by the ASRC Instrument at the Table Mountain Intercomparison: (a) two sequential scans near solar noon in log and linear ordinates, and (b) expanded central region of top.

let spectroradiometer) are the only instruments that have participated in both. A difficulty with reports of intercomparison results and accuracies is that they do not address how representative the intercomparison results are for routine long-term performance. We show the performance of the USDA reference ultraviolet spectroradiometer at Table Mountain in routine operation.

2 Spectroradiometer Performance

Figure 1 shows two terrestrial spectra taken with 0.1-nm (1 FWHM) sampling intervals at the 1997 North American UV Spectroradiometer Intercomparison (Table Mountain, Colorado).[10]

The solar scans in Fig. 1 were taken at 18:00 and 18:30 UCT on 17 September 1997, one of the two clear days during the Intercomparison. The 18:00 scan was close to local solar noon; we intentionally aborted it at wavelength 347 nm so we could make other measurements before the next scheduled scan starting at 18:30. The 18:30 scan continues to 360 nm. The instrument is capable of measuring to 410 nm, but the Intercomparison protocol did not permit us to do so. Our standard operating protocol makes uniform 1-sec integrations at stationary 0.1-nm (1 FWHM) steps, from short to long wavelengths. All of these control parameters are easily changed; this protocol is chosen for ease of data use. The lower panel shows a central region of the spectrum, so that the structure of the spectrum (and our ability to capture it) can be appreciated. Under these conditions, at all wavelengths greater than 295 nm the uncertainty due to Poisson statistics of photon counting is less than 5%, and less than 1% beyond 299 nm.

Figure 2 shows a typical observation (with a new Hg lamp) of the 296.728-nm emission line of mercury, observed by instrument U-111 at Table Mountain during the course of its post-midnight calibration scans. The solid trace shows the instrument slit function. The dotted trace shows the same data to emphasize that this signal is seen on a baseline of emission continuum, and that there is a weak
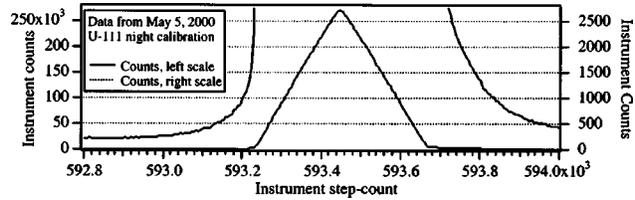

Fig. 2 Observation of the 296.728-nm emission line of Mercury.

side peak on this line to the right. (Identified by operating the instrument with slits adjusted to yield a FWHM of 0.01 nm, not shown.) This "tail" is not due to the instrument function.

The 296-nm line is commonly used as a calibration line for UV spectroradiometers because it is in the domain where wavelength accuracy is most needed. Most UV spectroradiometers have the resolutions closer to 0.6-nm FWHM or greater, and they cannot see small interferences like that evident in Fig. 2; nonetheless their wavelength assignments are affected by them.

3 Stray Light, Out-of-Band Rejection

The instrument slit-scattering function measured against a 50-mW HeCd laser (with postdispersion to remove bore-glow contribution) is shown in the two panels of Fig. 3. These measurements were taken in our laboratory before the Intercomparison, and required most of a day to accomplish. (Similar measurements were made at the Intercomparison, but the laser illuminator provided there was less powerful, and a fiber-optic beam transport was used that further limited the available light. The low optical power and limited integrating times necessary to accommodate the multiple instruments at the Intercomparison meant that the measurements taken there could not detect the far out-of-band (OOB) floor of the ASRC/USDA Spectroradiometer.)

In all practical monochromators, scattering from optical components, and secondarily from cavity surfaces, domi-
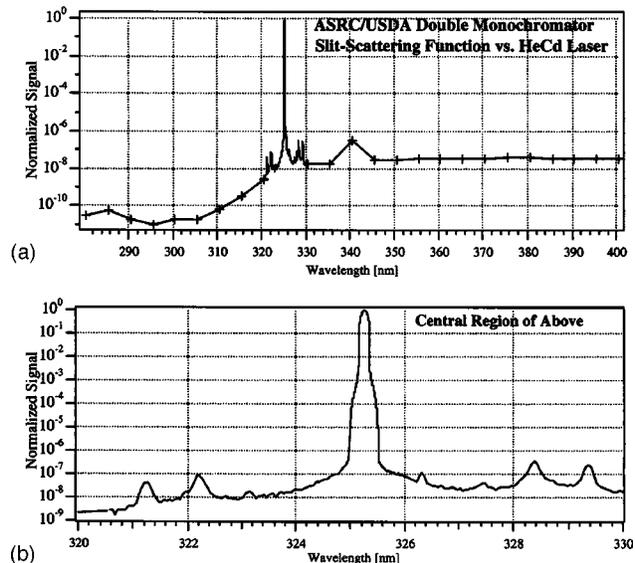

Fig. 3 (a) Extended slit-scattering function of ASRC/USDA spectroradiometer and (b) central region of same.

nate the tails of the stray light distribution, and the diffraction limit can only be approached for the region of the central peak. Given the dramatic increase in irradiance with wavelengths through the UVB (and persisting at the longer wavelengths) seen in Fig. 1(a), the critical optical performance issue for a UV spectroradiometer is the ability to reject unwanted light from all longer wavelengths. The extended slit-scattering function seen in Fig. 3(a) is a measure* of this; when measuring at wavelengths 310 nm and below, less than 10^{-10} of the light from 325 nm leaks through. When measuring at longer wavelengths, more stray signal is detected† ($\approx 2 \times 10^{-8}$), but this has no impact on terrestrial spectra because the irradiance being measured at this wavelength is so much greater than that at shorter wavelengths. Thus the far OOB rejection ratio of the ASRC/USDA Reference Spectroradiometer is better than $\approx 10^{-10}$, and the data at 290 nm in Fig. 1 are limited by the Poisson statistics of photon arrivals, but not by OOB. The dark-count rate of our instrument is a few counts per minute. We can run scan protocols, where integration time is set-controlled to produce uniform counts up to a time limit; with this, longer integrations are available at short wavelengths without increasing the total acquisition time for the spectrum. This permits routine measurements at 290 nm under most conditions. We believe this to be the best current performance for stray-light rejection in a UV spectroradiometer.

4 Angular Response

Figure 4 shows the angular response of the fore-optic. These data were taken with our automated angular response test bench; the fore-optic was operated with a coupled detector operating at the numerical aperture relayed to the monochromator. The detector was a UG-11 filtered GaP photodiode; with the Xenon arc illuminator the result is a relatively uniform spectral integral from 280 to 400 nm. Other tests not shown here show the angular response to be insensitive to wavelength within this range. The two curves are before and after the bare aluminum of the external shroud supporting the diffuser was black anodized before field service; these two are shown both as a check on potential changes due to loss of anodization in service and the reproducibility of our measurement.

5 Wavelength Registration and Accuracy

The standard instrument operating protocol captures the 296.728-nm (in air, at STP) emission line of Hg during each retrace following a solar scan, and most nights make a scan of multiple lines, of which the lines at 289.359, 296.728, 312.566, 334.148, 365.0146, 404.6561, and 407.781 nm (air, STP) are used for primary calibration.

---

*If the instrument responsivity is independent of wavelength, then the slit-scattering function is a direct measure of the out-of-band (OOB) rejection ratio. In this instrument, the responsivity falls modestly at short wavelengths due to both fore-optic efficiency and monochromator throughput, but not enough to affect the results materially when seen logarithmically over so many decades.

†We believe fluorescence and/or Stokes inelastic scattering (likely the cause of the ''peak'' at 15 nm from the stimulating wavelength) in the Lambertian fore-optic is responsible for the elevated floor of the slit-scattering function to longer wavelengths. It is nearly absent when measurements are made without the fore-optic.
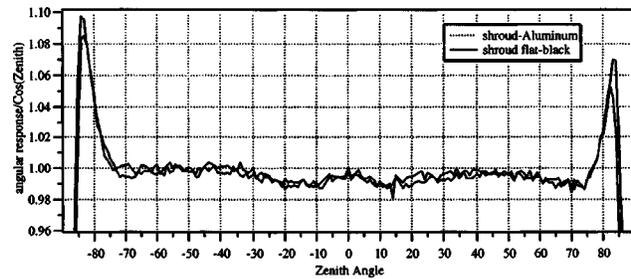

Fig. 4 Fore-optic angular response, error ratio versus cosine.

The most commonly used method of determining the center of an emission-line peak is to compute the center-of-moment of the distribution, after linear baseline subtraction. This has the virtue of being easy to code, fast, and able to work with arbitrary instrument slit functions and peak distributions. However, the moment centroid is far more vulnerable to signal noise, issues of base-line subtraction methods, and weak side lobes than better methods of peak-center recovery. In these data we show both method-of-moment and also dual-slope intercept results. The dual-slope intercept works well for a triangular slit function; it computes the peak center as the intersection of the two least-square fit-lines from 10 to 90% of peak amplitude, on the left and right. This result is independent of any linear baseline superimposed on the data. For the 296.7-nm line, there is an approximately 0.001-nm bias between the two estimators, with the dual-slope method yielding the lower value. This is due to the side lobe seen in Fig. 2, which biases the method-of-moment estimate upward. We use the dual-slope estimator for our wavelength calibrations.

Secondarily, the computation of both results provides an easy test for Hg lamp ignition difficulties. When the lamp ignition is delayed, the lamp output is still rising during the peak acquisition. In this condition the method-of-moments estimator diverges substantially from the dual-slope estimator. Figure 5(a) illustrates instrument wavelength registra-
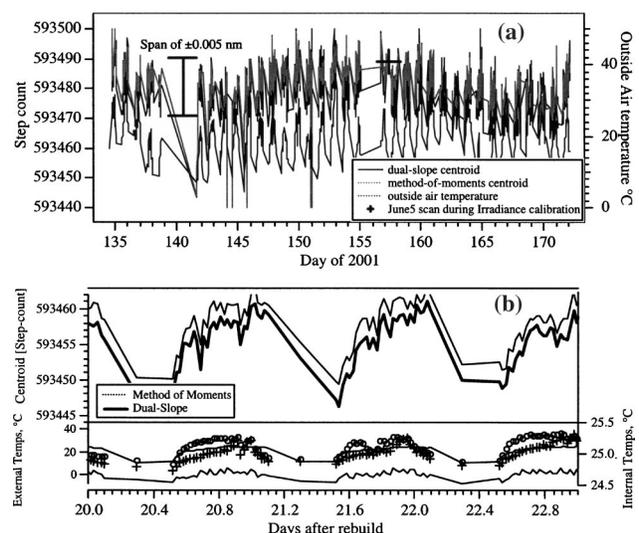

Fig. 5 (a) Time-series of 296-nm retrace centroids for May/June 2001 and (b) detail of retrace scans following lamp replacement on 29 April 2000.

tion reproducibility, processing, and instrument trend from the period 15 May to 22 June 2001. This period is the tail-end of 1.25 years of operation when the internal Hg calibration lamp is as degraded as we permit it to become. In interpreting these figures, note that to a very close approximation there are 2000 instrument steps per nanometer, and that the instrument is normally indexed so that step-count $\approx 2000 \times$ nm for convenience. The worst-case diurnal variability of approximately ± 0.005 nm is superimposed on a slower variation we attribute to barometric pressure. While not apparent at this scale, the divergences beyond the 0.005 limit are delayed ignition outliers, discriminated by the divergence of the two retrievals. These preferentially occur during cold conditions, and are much worse at the end of the Hg lamp lifetime as shown.

Figure 5(b) shows a higher time-resolution sample of what is effectively the same data, but taken from a time immediately after Hg lamp replacement when there are no ignition difficulties. The circles and crosses are the fore-optic temperature (measured at the photodiodes, just above the Hg lamp) and the outside air temperature, respectively, shown against the temperature ordinate on the left side of the graph. The fore-optic is hotter than the ambient air, both because it is black and receiving solar radiation, and because the periodic operation of the Hg lamp heats it. Two temperatures internal to the monochromator are shown with lines against the right ordinate, because these fluctuate much less. The dotted line is the temperature measured in the air within the instrument housing at the monochromator faceplate (entrance and exit slits), the solid line is the photomultiplier temperature, which is warmer due to its electrical dissipation, and less variable due to its heat capacity. Note that although the internal temperature variations are small ($\approx 0.2°C$ minimum to maximum in these data), they correlate well with the centroid perturbations. The direct effect of air temperature on the diffraction at the grating is too small (by more than an order of magnitude), to explain the variation. We conclude that the temperature variations are thermomechanically driving the slits/faceplate of the monochromator. Extensive runs of data such as those shown in Fig. 5(b), and more extensive measurements done at the 1997 North American UV Spectroradiometer Intercomparison (and also on our instruments while at ASRC), demonstrate that the variability is nearly uniform at all wavelengths, and yield a Pearson's correlation coefficient of 0.8 from retrace to retrace (meaning the correlation of scan data to the retrace is better). We use the 296-nm line observations from each retrace to detrend the solar spectra. The resulting estimated uncorrected variation in the assigned wavelength then becomes approximately ± 2.7 steps rms, or 0.00135 nm, yielding a U95 (i.e., 2σ) wavelength variation of 0.0025 nm for data corrected using the 296-nm retrace observations, when the Hg lamp ignites properly.

6 Wavelength Calibration Method and Algorithm

Wavelength calibrations are derived from the nightly high-resolution scans done of the internal Hg emission lamp. These scans capture the following emission lines, wavelengths are in nanometers (in air, at STP) from the Chemical Rubber Corporation (Cleveland)[11] and Reader, Sansonetti, and Bridges.[12] There are very close to 2000 steps/nm, and the instrument is indexed so that step count/2000 is
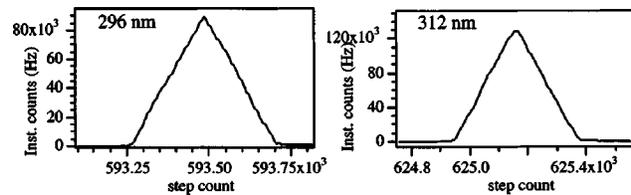

Fig. 6 Two Hg peaks from the midnight calibration scan, taken near the end of a Hg lamp working life.

approximately the wavelength.** As authorities differ, our assumed values with nominal step counts are shown here:

289.359	×2000	=578718—well-isolated calibration line
296.728	×2000	=593456—well-isolated calibration line
312.566	×2000	=625132—first of a triplet (the 312.566 line is used, the 313 pair is not)
334.148	×2000	=668296—well-isolated calibration line
365.0146	×2000	=730029—first of a multiplet; the first is used, the rest are not
404.6561	×2000	=809312—isolated calibration line
407.781	×2000	=815562—isolated calibration line, near instrument limit.

Figure 6 demonstrates that with age (July 2001) the Hg lamp fluctuated considerably more than it did when new (the lamp is starting to fail), but that the peak centrations are still usable from these data. The instrument slit function should not be assessed from these figures.

Each individual instrument has a small wavelength nonlinearity versus steps, which should be fitted for best accuracy at longer wavelengths. This nonlinearity arises from inevitable small mechanical errors of the zero-contact position of the sine bar, (which are instrument specific and highly reproducible so long as the instrument is not rebuilt) and is a common feature of sine-drive instruments. The wavelength is proportional to $\sin(\theta)$, where θ is the grating angle from the zero order. In the presence of a small offset angle ε, the wavelength becomes $\sin(\theta+\varepsilon)$, which is well approximated for small ε as a second-order polynomial, which is the common approach.

A quadratic least-squares fit is done using the dual-slope centroid values with the line wavelength as the independent variable, because it is taken as absolute, and the instrument centroids in step counts are assumed to contain the variance to be minimized. When plotted (not shown), the deviation of the polynomial fit from a straight line cannot be seen by the eye.

$$\text{steps} = C_0 + C_1(\text{wavelength}) + C_2(\text{wavelength})^2$$

yields $C_0 = 500.4185166$, $C_1 = 1996.788271$,

$C_2 = 0.005495554781$ for 5 June 2001.

**The retrieved results show $d(\text{steps})/dl$ evaluated at 296.7 nm $= C1 + 2 \times C2 \times 296.7 = 1996.788 + 2 \times 1.631 = 2000.049$ steps/nm.

For the end-of-life Hg lamp data taken in July 2001, the worst-case variances from the fit correspond to ≈ 0.0025 nm, and this is approximately three times worse than we do with a more stable lamp. This estimates the precision of the fit; the absolute accuracy of individual determinations in continued operation is controlled by other effects discussed shortly.

To use this fit operationally, we solve the quadratic equation to yield the instrument wavelength λ(nm, air, STP) $= \{ -C_1 \pm \text{SQRT}[C_1{}^*C_1 - 4^*(C_0 - \text{steps})^*C_2] \} / (2^*C_2)$. Only the root yielding positive wavelength is relevant.

To use these results in practice, for best accuracy we apply the local wavelength shifts diagnosed from the 296-nm retrace lines, when available. Figure 5(a) shows the time series of the 296-nm retrace scans (taken only during the daytime) for the data from 14 May to 20 June 2001. The optional automated 296-nm retrace protocol ignites the Hg lamp when the "forward" scan is finished at its longest wavelength, the monochromator is slewed backward to 296.5 nm, the Hg line is scanned forward at 10-step resolution (0.02 nm), and then the mechanical retrace is resumed to preposition the grating for the next operational scan. This protocol adds approximately 2.5 min to the measurement cycle time.[‡] Diurnal variation associated with ambient temperature (note correlation with the outside air temperature plotted later, with scale to right) is apparent. Secondarily, a weak variation can be seen, which we attribute to barometric pressure. The full envelope of the wavelength variation is ± 0.005 nm.

The availability of the 296.7-nm retrace scans allows these variabilities to be corrected in the processed data by computing steps$'$ = steps$- (\text{Hg}296 - 593487.2)$ where "steps" is the sine-drive step count for the observation in question, and Hg296 is the dual-slope centroid value of the preceding 296-nm retrace if available. The constant in the above expression is the polynomial-fit step value for the 296.728-nm line. Substituting steps$'$ into the calibration equation for λ then yields wavelengths corrected for the local offset apparent in Fig. 7.

With this method, the uncorrected wavelength variability is driven well below 0.0025 nm. The absolute accuracy is then controlled by the absolute accuracy of the wavelength calibration itself (including both residuals and accuracy of the line constants) and the residual sinusoidal errors we measured as part of our efforts associated with the 1997 Table Mountain intercomparison. We believe that the absolute wavelength accuracy of the measurements is limited by these systematic residuals, and is no worse than 0.005 nm. We have not corrected the data for the sinusoidal residual seen in 1997, because we are not certain they have remained stable for four years and several instrument moves. It requires an elaborate series of line-lamp measurements to fit them. We hope to redo these later and may then revise wavelength assignments slightly.

[‡]The observation of the 296.7-nm Hg emmission line done optionally during the retrace period of solar observations could be done faster if it were made in the reverse direction, but we are concerned about the potential for mechanical hysterisis. We have made measurements of reverse direction scans showing no discernable hysterisis, but we do not want to depend on this persisting through the full instrument operating life.
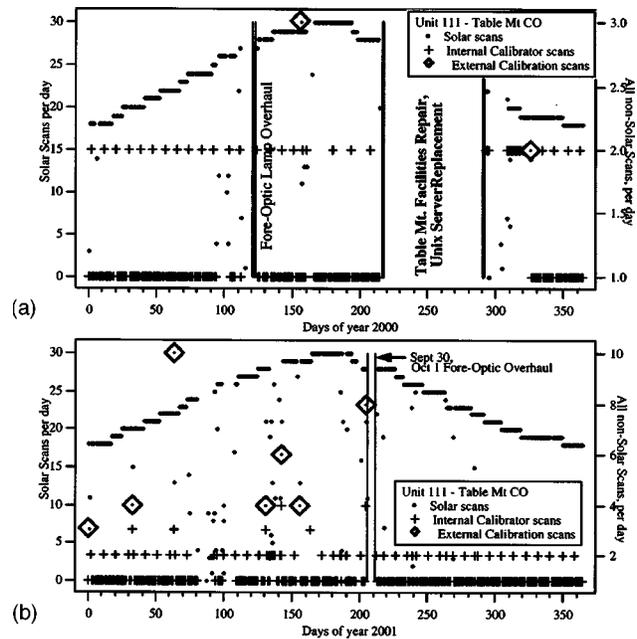

Fig. 7 Operational status in (a) 2000 and (b) 2001.

The operating history of U-111 at Table Mountain is shown in Fig. 7. For data-quality purposes there are four epochs: prior to 30 April 2000, from 1 May to 1 August, and then from 19 October through to the end of the year and continuing to the fore-optic rebuild of 30 September 2001, and then the remainder. During the winter of 1999 to 2000 the cold-start conditions on the internal Hg calibration lamp (in the instrument fore-optic, and hence affected by ambient temperature) degraded its ignition reliability and light output to the point that the wavelength registrations in the earliest data in 2000 are marginal. The instrument received periodic maintenance from 25 to 29 April 2000, entering the fore-optic to replace the aging Hg lamp, and replacing the C01 internal calibrator bulb. After this, wavelength registration was excellent; with decaying but acceptable performance throughout these data to the subsequent fore-optic and lamp overhaul in late September 2001.

In Fig. 7 the upper sinusoidal line of dots marks the annual cycle of daylight: the instrument will take a solar scan every half hour during daylight. The rarer points below this envelope show days where prolonged power outages prevented a full day's data accumulation. Internal irradiance calibrations are shown with a plus sign, and the external calibrations by the Central Ultraviolet Calibration Facility (CUCF, NOAA) are shown with a diamond. A much longer outage due to a facilities and infrastructure overhaul of the Table Mountain site occurred from 8 September through 18 October 2000. The instrument was not altered or directly affected during the facilities repair, but internet communication was not available for two weeks. Following this interruption, the unix computer, which handled the instrument data, was discovered to be erratic and failing, and the remainder of the data loss was associated with obtaining a replacement, and getting it installed and configured.

Following this outage, the instrument has operated steadily to date. During summer 2001, extensive UV instru-

ment intercomparisons were held at Table Mountain. For this reason we delayed maintenance on the instrument until 30 September 2001. We want to emphasize that in contrast to many instrument intercomparisons where the instruments in question have been specially prepared and are attended throughout an intercomparison, our USDA reference instrument ran routinely without special attention, and was in a condition certainly more representative of long-term operation than is typical for intercomparisons.

On 30 September and 1 October 2001, the fore-optic of our instrument was overhauled again: a new diffuser/integrating cavity was installed, and the internal Hg emission lamp was replaced. A variety of system improvements were added, including a thermostatic heater to the upper fore-optic to improve Hg lamp life-time by eliminating the cold-start problem, external hardware interfaces to support a portable external calibrator we have devised, and new firmware accommodating this and other upgrades.

During 2001, the instrument yielded 90% data availability of scheduled solar scans, discounting three days of intentional outage for the fore-optic overhaul. This 90% statistic is not corrected for loss of availability due to external irradiance calibrations, which for operator convenience are generally done during daylight hours. The primary cause of data loss at Table Mountain is electrical power outages. Two clusters of data loss in April 2001 were associated with unix and internet issues not in any way caused by instrument performance.

7 Irradiance Calibrations; Instrument Responsivity

An irradiance-responsivity calibration is shown in Fig. 8. U-111 at Table Mountain receives direct calibrations from the NOAA CUCF facility. Responsivities are calculated by computing the interpolated "values" of the measurements at the exact 1-nm wavelengths of the lamp calibration tables as supplied by CUCF, subtracting the interpolated "mean instrument shutter," (a separate observation where the fore-optic is blocked to assess contribution to the irradiance from scattered light in the calibrator, a correction of approximately 0.6%) subtracting an instrument dark-count rate of 0.625 instrument Hz taken from multiple 10-sec integrations (yielding a negligible 0.065% greatest correction at 285 nm), and then dividing this result by the stated lamp irradiance in mW/m^2/nm from the NIST/CUCF table.
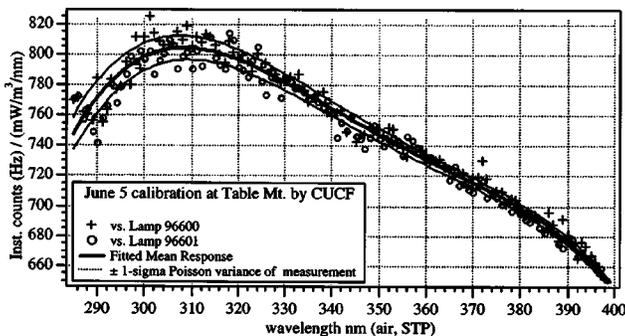
The Hg-296-nm retrace centroid for these calibrations is taken to be 593,481, from measurements made before, after, and during the CUCF calibrations.

The agreement of the two lamps' responsivities is remarkable, and within the evident sample-to-sample noise figure at all wavelengths. The standard deviation of individual measurements from either lamp from a fitted or smoothed line is approximately 5 instrument Hz/(mW/m^3/nm), where the instrument's responsivity is 760 to 790 in this range, yielding 0.65%. This is congruent with the expectation value for the Poisson variance due to the finite number of counted photons shown in the graph.

Given no reason to prefer one or the other of the two lamps, we show a mean responsivity for both of them, and then a fourth-order polynomial fitted to the mean response, for this particular data,

$$Responsivity = -103072.3223 + 1189.7654673\lambda$$
$$-5.09178173443\lambda^2$$
$$+0.00965826022932\lambda^3$$
$$-6.86067549928e\text{-}06\lambda^4,$$

where responsivity is in the units of instrument Hz/(mW/m3/nm) and λ is the wavelength in nanometers (air, STP). These variances are such that the polynomial form can be considered as fully representing the data we have, with the only possible discrepancy being the apparent dip around 345 nm. On the basis of our measurements against other sources, we believe that the spectrometer does not have a feature in its responsivity here. If this is so, then the fitted results are more accurate in this domain than the raw data.

Data users should note that the form of the responsivity shown here is what we expect from other measurements and instrument design considerations. This includes the apparent downward inflection point at 390 nm. This is a consequence of the first grating starting to overfill as the grating tip angle increases past this wavelength. (The grating no longer captures all the light in the system numerical aperture.)
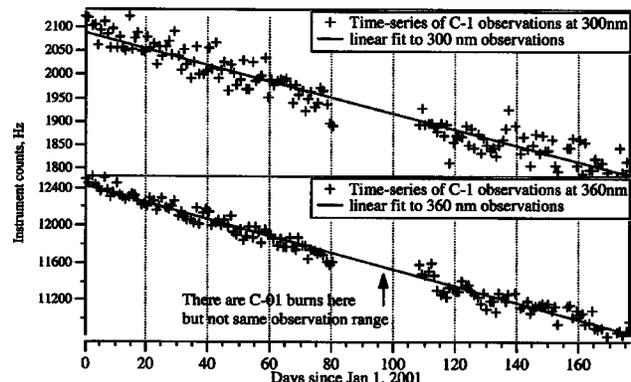

Fig. 8 Instrument responsivity from CUCF calibration.

Fig. 9 Internal calibrator trends in instrument response plus lamp output in the first half of 2001.

Fig. 10 Internal calibrator trends versus wavelength in nanometers.

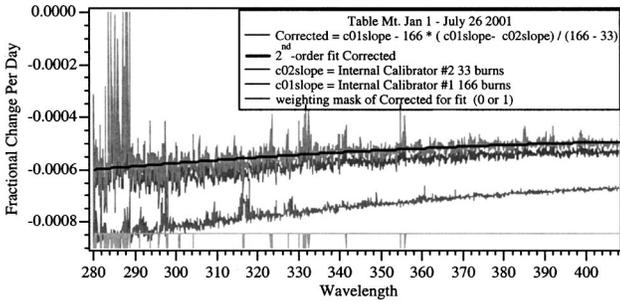**Fig. 11** External CUCF portable calibrator trends versus wavelength, in nanometers.

8 Trends in Instrument Responsivity

Following the site-rework outage of Fall 2000, instrument U-111 has received CUCF irradiance calibrations on 21 November 2000, and then in 2001 on 2 January, 2 February, 5 March, 11 and 23 May, 5 June, 24 July, 1 October (after a fore-optic and lamp rebuild), and then 11 January 2002. From these repeated calibrations, we observe a downward trend in the instrument responsivity, interrupted with a discontinuity by the fore-optic element exchange of 30 September 2001. The routine data production depends on both the CUCF external calibrations, and the much more frequent responsivity checks from the internal irradiance calibrators.

The instrument has two independent 20-W halogen bulbs in the fore-optic below the entrance element, designated C-1 and C-2. These can be used alternately driven by a single precision current supply. A solenoid-driven diffuse target is interposed to return the lamp output along the optical path to the spectrometer. The lamps are intentionally used at different operating frequencies; calibration checks against C-1 are typically done every night. C-2 is used more sparingly, of late once every nine days. Figure 9 shows the downward trend in raw instrument response (plus decay of lamp output) at two wavelengths from the more numerous C-1 observations, from 1 January to 5 June of 2001. As can be seen, the trends are very steady and consistent. We had hypothesized that the downward trend was due to oxidation of interior optical elements, and so in February (day 50 in this figure), the instrument was switched to a N_2 purge supply. As is apparent, this was not palliative, though we continue this for U-111 to avoid the introduction of new variables.

The least-squares linear trend with time observed in the C-1 and C-2 scans for individual wavelengths (e.g., Fig. 9), are shown for all wavelengths in Fig. 10. The inset table identifies the lines from top to bottom in order within the figure, except for the second-order fit. The raw data from the numerous C-1 observations show the largest negative trend, the next curve above show the fits from the less frequent (and hence the fit is noisier) C-2 data. With the assumption that this trend for each lamp's observations is a linear sum of a trend in the instrument responsivity itself, and a decay trend of the lamp which is proportional to the usage, we can solve for the instrument trend independent of lamp decay, seen above it. This is a relatively small correction to the C-2 observations, and noisier yet due to the subtractions. The heavy black line is a quadratic fit through these corrected operations, with a noise weighting mask
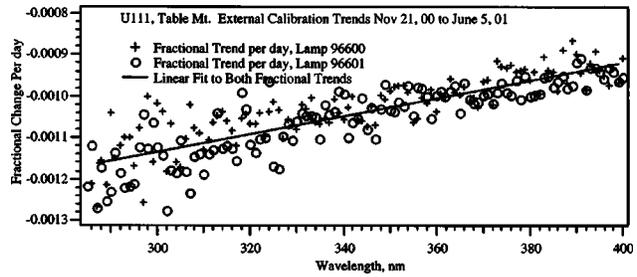
(either 0 or 1) to discard outliers beyond 2 standard deviations, shown at the bottom. The inferred trend of $\sim$ -0.00055 per day (at 340 nm, the mid-wavelength point) compounded would yield -18.2% per year.

This figure should be contrasted to Fig. 11, which shows the trend retrieved against the two external FEL lamps (96600 and 96601) from the five external calibrations over a similar period. Note that the external trends versus the FELs are apparently twice the internal calibrator trend. Repeated calibrations of the CUCF-held lamps 96600 and 96601 demonstrate their stability over this epoch. Hence we believe fore-optic throughput is responsible for approximately half the total trend (the internal calibrators do not exercise the fore-optic). Despite this large trend, we can provide accurate data because it is well behaved.

After the summer intercomparisons, the instrument fore-optic was replaced during maintenance done on 30 September 2001. Figure 12 shows the ratio of the measured signal from the two CUCF external calibrations done subsequently, each calibration exposed lamps 96601. In comparing this figure against the previous two figures, be careful of the differing ordinates (without adequate numbers of repeat calibrations, the LS slope fits done for earlier figures are not useful); the change in the responsivity at 300 nm in Fig. 13 corresponds to $-0.225/114 = -0.0019$ per day as presented in Fig. 11. Thus after the replacement with a new fore-optic, the trend in responsivity is slightly larger. For brevity only the internal CO-1 trends are shown in Fig. 13. Note that these are slightly smaller than before, and thus contribute a smaller effect to the total trend and have an apparent opposite sensitivity to wavelength.

9 Conclusions

The USDA reference spectroradiometer has met the goal of providing high resolution UV radiometric observations on a
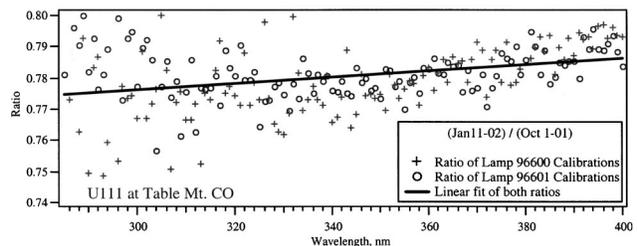

Fig. 12 Ratio of CUCF portable calibrations after the fore-optic replacement, 30 September 2001.
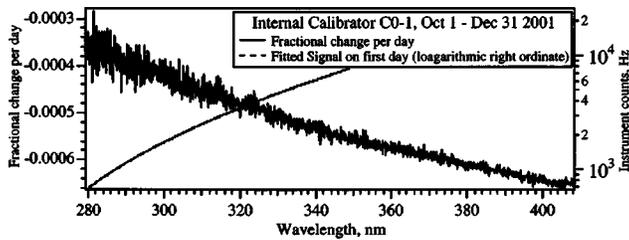
Fig. 13 Internal calibrator C-1 trends versus wavelength in nanometers (with new fore-optic).

continuing long-term basis at a rarely attended field site. The instrument has operated for more than a year without internal maintenance and delivered high-accuracy data when tested by an independent intercomparison.

We believe these instruments to be the highest resolution, and best out-of-band rejection, field spectroradiometers for the ultraviolet in routine operation. These instruments have met all the specifications set for them by the original development goal, and easily meet the S-2 instrument goals specified by WMO/GAW for ultraviolet spectroradiometers.[7] We meet all of their specifications in routine operation except the 10-min scan. The instrument is capable of doing so; we operate at present with uniform 1-sec integrations at all wavelengths (rather than allowing the integrations at longer wavelengths to be set by photon counting statistics, which shortens them considerably) in the interest of ease of use of the data.

However, improvement in the stability of instrument responsivity (not a specification in the WMO report) would clearly be desirable. The current trends require multiple calibrations per year and careful data processing to make the data useful. It is apparent that fore-optic aging dominates this trend; with a secondary contribution from internal throughput and photomultiplier quantum efficiency, we cannot disaggregate at present. The trend due to fore-optic aging and soiling is modestly greater with a new fore-optic compared to one well aged *in-situ*, but not remarkably so.

Efforts are underway at present to make the fore-optic more stable with age, and to understand and reduce the trends in responsivity. We have also recently introduced a set of external portable calibrators, which can be operated and transported more easily than the CUCF calibrator; the maintenance and transfer of the calibrations to the other sites depends on these. We have not yet gained sufficient statistics to report their performance.

Progress in these efforts will reduce the need for external calibrations, and ease data handling. At present the instrument data can be delivered and detrended to an irradiance reproducibility specification of $<0.7\%$ (1σ) from the CUCF calibration ensemble from November 2000 through September 2001. Uncertainty will be larger for the early epoch following the fore-optic replacement of 30 September ber 2001 to date, in part because of the increased trend in fore-optic throughput. Because we have only the three full external calibrations, we cannot formally state an expectation for the increased uncertainty in this epoch but it will not double. We expect this to return to a comparable value shortly with fore-optic age and as we acquire further calibrations. This statement of uncertainty does not consider any potential error in the CUCF lamp irradiance scale.

References

1. J. Herman, R. L. McKenzie, S. B. Diaz, J. B. Kerr, and G. Seckmeyer, "Surface ultraviolet radiation, in scientific assessment of ozone depletion 1998," Chap. 9, World Meteorological Organization, Global Ozone Research and Monitoring Project, Report No. 37, UNEP, P.O. Box 30552, Nairobi, Kenya (1999).
2. V. E. Fioletov, J. B. Kerr, E. W. Hare, G. J. Labow, and R. D. McPeters, "An assesment of the world ground-based total ozone network performance from the comparison with satellite data," *J. Geophys. Res., [Atmos]* **104**, 1737–1747 (1999).
3. T. F. Eck, P. K. Bhartia, and J. B. Kerr, "Satellite estimation of spectral UVB irradiance using TOMS derived total ozone and UV reflectivity," *Geophys. Res. Lett.* **22**, 611–614 (1995).
4. G. Seckmeyer, B. Mayer, G. Bernhard, R. L. McKenzie, P. V. Johnston, M. Kotkamp, C. R. Booth, T. Lucas, T. Mestechkina, C. R. Roy, H. P. Gies, and D. Tomlinson, "Geographical differences in the UV measured by intercompared spectroradiometers," *Geophys. Res. Lett.* **22**, 1889–1892 (1995).
5. V. E. Fioletov, L. J. B. McArthur, J. B. Kerr, and D. I. Wardle, "Long-term variations of UVB irradiance over Canada estimated from Brewer observations and derived from ozone and pyranometer measurements," *J. Geophys. Res., [Atmos]* **106**, 23009–23027 (2001).
6. J. Grobner and J. B. Kerr, "Ground-based determination of the spectral ultraviolet extraterrestrial solar irradiance: Providing a link between space-based and ground-based solar UV measurements," *J. Geophys. Res., [Atmos]* **106**, 7211–7217 (2001).
7. G. Seckmeyer, Editor. "Instruments to measure solar ultraviolet radiation Part 1: Spectral instruments," G. Seckmeyer, Ed., World Meterological Organization Report 125, WMO TD 1066.
8. G. Bernhard and G. Seckmeyer, "Uncertainty of measurements of spectral solar UV irradiance," *J. Geophys. Res., [Atmos]* **104**, 14321–14345 (1999).
9. A. F. Bais, B. G. Gardiner, H. Slaper, M. Blumthaler, G. Bernhard, R. McKenzie, A. R. Webb, G. Seckmeyer, B. Kjeldstad, T. Koskela, P. Kirsch, J. Gröbner, J. B. Kerr, S. Kazadzis, K. Leszczynski, D. Wardle, C. Brogniez, W. Josefsson, D. Gillotay, H. Reinen, P. Weihs, T. Svenoe, P. Eriksen, F. Kuik, and A. Redondas, "The SUSPEN intercomparison of ultraviolet spectroradiometers," *J. Geophys. Res., [Atmos]* **106**, 12509–12526 (2001).
10. K. Lantz, P. Disterhoft, J. DeLuisi, E. Early, A. Thompson, J. Berndt, L. Harrison, P Kiedron, J. Ehramjian, G. Bernhard, L. Cabasug, J. Robertson, W. Mou, T. Taylor, J. Slusser, D. Bigelow, B. Durham, G. Janson, D. Hayes, M. Beaubien, and A. Beaubien, "The 1997 North American interagency intercomparison of ultraviolet spectroradiometers including narrowband filter radiometers," *J. Res. Natl. Inst. Stand. Tech.*, (in press).
11. *Handbook of Chemistry and Physics*, 23d ed., Chemical Rubber Corp., Cleveland OH.
12. J. Reader, C. J. Sansonetti, and J. M. Bridges, "Radiances of spectral lines in mercury pencil lamps," *Appl. Opt.* **35**, 78 (1996).

Biographies and photographs of the authors not available.